PHYSICAL REVIEW B VOLUME 55, NUMBER 11 15 MARCH 1997-I

Perturbative approach to high-energy-electron surface-resonance scattering

P. M. Derlet and A. E. Smith
Department of Physics, Monash University, Clayton, Victoria 3168, Australia

(Received 11 October 1996; revised manuscript received 2 December 1996)

Recently, an exact expression has been developed to determine the elastic reflection coefficient for the phenomenon of surface resonance in reflection high-energy-electron diffraction [S. L. Dudarev and M. J. Whelan, Phys. Rev. Lett. **72**, 1032 (1994)]. Following this proposal, diagrammatic techniques are used to obtain a series expansion for the resonant reflection coefficient with respect to an array of noninteracting Breit-Wigner scatterers. Application to the (111) surface of platinum within the weak-potential scattering regime reveals, within the uncertainty of the scattering parameters, that only the lowest-order result is required. This disputes the contention (in this case) that the Breit-Wigner scattering law is violated. From an analysis of the convergence properties of the series, it is found that this is due primarily to incoherent resonant scattering within the bulk between the (111) planes. In turn, its origin is the off-Bragg scattering condition associated with weak-potential scattering. On the other hand, for the case of strong-potential scattering in which the Bragg condition is satisfied, the perturbation series breaks down and the exact solution is needed. We then develop a renormalized perturbation expansion with respect to the Breit-Wigner scattering vertex in the intermediate regime, where there is still strong-potential scattering. Correspondingly, a more general convergence criterion is determined. We conclude by showing that the developed perturbation expansion and convergence criterion retain their form for an arbitrary number of interacting resonant modes. [S0163-1829(97)02512-5]

I. INTRODUCTION

With improving experimental techniques, reflection high energy electron diffraction (RHEED) and reflection electron microscopy (REM) have reemerged as methods capable of providing information on surface structure and growth (for a review, see Ref. 1). Owing to the strength of the interaction potential, electron diffraction is inherently ‘‘dynamical,’’ as opposed to say x-ray diffraction. That is to say, in general there are many closely coupled diffraction states. Accordingly, the problem is computationally intensive with many states closely coupled and hence dense matrices are required to be dealt with. This increases the difficulty of ‘‘inverting’’ results to determine crystallographic (structural) data from the combination of experimental data with computation.

The elastic transmission case has, however, been adequately dealt with for many years.[2,3] In this case only the forward scattering amplitude is needed and thus the full three-dimensional (bulk) Schrödinger equation is retained. This gives a series of coupled algebraic equations over all reciprocal lattice vectors parallel to the direction of the surface. Great insight in the transmission case can be provided by the use of the so-called ‘‘two beam’’ approximation corresponding to two scattering states (i.e., the incident beam together with one diffracted beam). The resulting 2×2 matrix is essentially the simplest nearly free electron or pseudopotential method of solution which can afford a simpler yet greater insight than mere computation.

For the case of RHEED, on the other hand, the surface geometry plays a greater role since it is a reflection technique and precludes such a simple approach. To gain a similar physical insight into the diffraction phenomenon, the ‘‘two beam’’ approximation must be replaced by the ‘‘two rod’’ approximation. In this, a pair of coupled differential equations rather than a pair of coupled algebraic equations, as in the transmission case, must be solved for, to fully take into account the backscattered amplitudes so important to the reflection phenomenon.

A typical RHEED pattern contains a range of diffraction phenomena. The direct Bragg scattering spots arising from the surface and bulk periodicity are compounded by secondary Bragg scattering of inelastically scattered electrons, the so-called Kikuchi lines and envelope.[4] These features primarily arise from potential scattering: the diffracted beam reflecting back into the vacuum. Additionally, there is the case where the scattered beam has a complex wave-vector component perpendicular to the surface and is therefore an evanescent wave propagating parallel to the surface. In this case the corresponding diffraction spot disappears from the screen. For certain incident electron energies and directions, such evanescent modes can be close in energy to bound electronic state(s) within the crystal. This results in an increase of the coupling between the specular and evanescent components, and therefore an associated increase in the intensity of the former. It is such an increase in the specular intensity that in the present context it is referred to as ‘‘resonance scattering.’’[5–7] This appears on a RHEED pattern as a parabola and is often referred to as a ‘‘resonance parabola.’’ In general a number of such parabolas exist, each corresponding to a two-dimensional reciprocal-lattice vector that forms the real part of the wave vector for the (evanescent) propagation mode. When such resonance parabolas intersect horizontal Kikuchi lines or, indeed, the first-order diffraction spots, there is a large increase in intensity in these directions, corresponding to an improved contrast in the resulting surface image.

There has been much debate as to the nature of the electronic state(s) that are involved in this resonance phenomenon. Early theoretical work[8,9] takes the view that surface states play the primary role. However, for the case of atomi-

0163-1829/97/55(11)/7170(11)/$10.00

cally flat crystal surfaces it has been conjectured[10,11] that such resonances arise from multiple scattering primarily within the bulk of the solid. In an illuminating series of recent papers, Dudarev and Whelan[12–15] have succeeded in establishing analytic techniques to consider this aspect of the surface diffraction problem. In particular, by mapping the resonance scattering process onto the one-dimensional semi-infinite tight binding Hamiltonian, they determine an exact analytical expression for the resonant reflection coefficient for the case in which there is minimal potential scattering[12–14] and for the case of arbitrarily strong potential scattering[15] corresponding to an intersection between a horizontal Kikuchi line and a resonance parabola. We note that in their calculation, as in the present work, the calculated electron intensities are presented as a function of incident electron direction. In a realisitic RHEED spectrum, the extent of the contribution of such a component will be a function of the electron distribution due to convergent beam RHEED (CB-RHEED) conditions and/or inelastic scattering (i.e., thermal diffuse scattering or phonon scattering). This aspect is not considered in the present model: the calculated intensities are decoupled from the inelastic processes and cannot be compared to the *primary* Bragg-scattered peak intensities.

In this paper we will show how Dudarev and Whelan's approach can be recast and further clarified by the use of diagrammatic techniques that have been applied to a wide range of phenomena.[17] In addition, we demonstrate how the resonance reflection coefficient can be expressed as a series expansion with respect to an array of noninteracting planes (parallel to the surface) each of which is of the Breit-Wigner scattering form. In Sec. II, we introduce the standard ''two rod'' approximation in its integral form, and following Dudarev and Whelan, we choose the form of the crystal electronic Green's functions under the assumption of minimal potential scattering. In Sec. III, a discrete integral equation is derived via an iterative process, the solution of which can be used to obtain the resonant reflection coefficient. Section IV contains the evaluation of the reflection coefficient for the simple cases of a single scattering plane and an array of noninteracting scatterers, giving the standard Breit-Wigner form. Using diagrammatic techniques, a perturbation expansion with respect to the Breit-Wigner form is then developed and its validity investigated. In Sec. V, we compare our perturbative calculation to the exact analytical result of Dudarev and Whelan for the case of the (111) surface of platinum. In Sec. VI we consider the perturbative approach in the strong potential scattering regime and develop a general convergence criterion. Lastly, in Sec. VII, the more general interacting N-''rod'' case is investigated. It is demonstrated that if the underlying assumptions of the Dudarev and Whelan approach are retained, then the perturbation expansion is simply renormalized by the additional many-beam interactions, thus extending the developed convergence criterion beyond the ''two rod'' approximation.

II. THE RESONANCE EQUATIONS

For a plane-wave electron with wave vector $\mathbf{k}$, incident on a semi-infinite crystal, the full crystal Schrödinger equation can be Fourier transformed in the plane parallel to the surface to give a series of second-order coupled differential equations:[16]

$$-\frac{\hbar^2}{2m}\frac{d^2}{dz^2}\Psi_{\mathbf{g}}(z)+\sum_{\mathbf{g}'}U_{\mathbf{g}-\mathbf{g}'}(z)\Psi_{\mathbf{g}'}(z)=\frac{\hbar^2k_{\mathbf{g}}^2}{2m}\Psi_{\mathbf{g}}(z). \tag{1}$$

$U_{\mathbf{g}}(z)$ and $\Psi_{\mathbf{g}}(z)$ are the two-dimensional Fourier transforms of the three-dimensional crystal potential $U(r)$ and the electronic wave function $\Psi(z)$. The $\mathbf{g}$ constitute the two-dimensional reciprocal-lattice vectors of the crystal structure parallel to the surface, and $k_{\mathbf{g}}^2=k^2-(\mathbf{k}_{\|}+\mathbf{g})^2$, the energy $\hbar^2k_{\mathbf{g}}^2/2m$ being associated with the motion of the electron normal to the surface. For a negative energy value (complex $k_{\mathbf{g}}$) this mode corresponds to an evanescent wave propagating in a direction parallel to the surface. We note that the equation for $k_{\mathbf{g}}$ defines the resonance parabola for a given $\mathbf{g}$ and can be seen by plotting k_z versus $|\mathbf{k}_{\|}|$.[14]

Within the ''two rod'' approximation where only two ''states'' are considered, the Schrödinger equation decouples into the two equations,[12]

$$\begin{aligned}
&-\frac{\hbar^2}{2m}\frac{d^2}{dz^2}\Psi_0(z)+U_0(z)\Psi_0(z)\\
&\quad+U_{-\mathbf{g}}(z)\Psi_{\mathbf{g}}(z)=\frac{\hbar^2k_0^2}{2m}\Psi_0(z),\\
&-\frac{\hbar^2}{2m}\frac{d^2}{dz^2}\Psi_{\mathbf{g}}(z)+U_0(z)\Psi_{\mathbf{g}}(z)\\
&\quad+U_{\mathbf{g}}(z)\Psi_0(z)=\frac{\hbar^2k_{\mathbf{g}}^2}{2m}\Psi_{\mathbf{g}}(z),
\end{aligned}\tag{2}$$

the integral form of which is

$$\Psi_0(z)=\Psi_{k_0}^{+}(z)-\int dz'G\left(z,z',\frac{\hbar^2k_0^2}{2m}\right)U_{-\mathbf{g}}(z')\Psi_{\mathbf{g}}(z'), \tag{3}$$

$$\Psi_{\mathbf{g}}(z)=\int dz'G\left(z,z',\frac{\hbar^2k_{\mathbf{g}}^2}{2m}\right)U_{\mathbf{g}}(z')\Psi_0(z'), \tag{4}$$

where $G(z,z',E)$ is the 1D electron Green's function connecting z and z' at an energy E. In Eq. (3), the wave function $\Psi_{k_0}^{+}(z)$ is defined by the one-dimensional Schrödinger equation

$$-\frac{\hbar^2}{2m}\frac{d^2}{dz^2}\Psi_{k_0}^{+}(z)+U_0(z)\Psi_{k_0}^{+}(z)=\frac{\hbar^2k_0^2}{2m}\Psi_{k_0}^{+}(z). \tag{5}$$

Here $U_0(z)$ is seen as the laterally averaged (semi-infinite) crystal potential.

Within the present work, we primarily consider scattering geometries which are far away from the Bragg condition in the direction perpendicular to the surface. Then scattering directly from the 1D crystal potential, $U_0(z)$, is minimal and the presence of the crystal can be represented simply by a complex wave vector, κ ($|\kappa-k_0|\ll|\kappa|$), the imaginary part of which characterizes the attenuation due to the potential. The solutions therefore obey the asymptotic conditions

$$\Psi^{+}_{k_0}(z)=\exp(ik_0z)+R_{\rm pot}\exp(-ik_0z)\qquad\text{for } z\rightarrow-\infty \tag{6}$$

and

$$\Psi^{+}_{k_0}(z)=\exp(i\kappa z)\qquad\text{for } z\rightarrow\infty, \tag{7}$$

where $R_{\rm pot}$ is the reflection coefficient due entirely to the crystal potential. Under these circumstances the free 1D Green's functions can be used. That is,

$$G\left(z,z',\frac{\hbar^2k_0^2}{2m}\right)=-i\frac{m}{\hbar^2\kappa}\exp(i\kappa|z-z'|)\qquad\text{for } z,z'\rightarrow\infty \tag{8}$$

and

$$G\left(z,z',\frac{\hbar^2k_0^2}{2m}\right)=-i\frac{m}{\hbar^2\kappa}\exp(-ik_0z+\kappa z')$$
$$\text{for } z\rightarrow-\infty\ \text{ and } z'\rightarrow\infty. \tag{9}$$

If we assume that the (bulk or surface) electronic state which contributes to the resonance phenomenon is approximately dispersionless, that is, the states are strongly localized at the their sites, then the resonant part of the Green's function can be given by a linear sum over the sites,[18] i.e.,

$$G\left(z,z',\frac{\hbar^2k_{\mathbf{g}}^2}{2m}\right)=\sum_n\frac{\phi_n(z)\phi_n^{\dagger}(z')}{\hbar^2k_{\mathbf{g}}^2/2m-\epsilon_0+i\Gamma_{\rm in}/2}, \tag{10}$$

where $\phi_n(z)$ is the localized state at site n, ϵ_0 is the on-site energy, and $\Gamma_{\rm in}$ the inelastic width of the "flat" dispersionless band.[12]

III. DERIVATION OF THE RESONANT SCATTERING REFLECTION COEFFICIENT

Substitution of Eqs. (6)–(10) into the integral equations (3) and (4) gives

$$\Psi_0(z)=\exp(i\kappa z)-\frac{im}{\hbar^2\kappa}\times\int dz'\exp(i\kappa|z-z'|)U_{-\mathbf{g}}(z')\Psi_{\mathbf{g}}(z'), \tag{11}$$

$$\Psi_{\mathbf{g}}(z)=\frac{1}{\hbar^2k_{\mathbf{g}}^2/2m-\epsilon_0+i\Gamma_{\rm in}/2}\times\sum_n\phi_n(z)\int dz''\phi_n^{\dagger}(z'')U_{\mathbf{g}}(z'')\Psi_0(z''), \tag{12}$$

and combining these to form an integral equation for $\Psi_0(z)$, we have

$$\Psi_0(z)=\exp(i\kappa z)-a\int dz'\exp(i\kappa|z-z'|)U_{-\mathbf{g}}(z')\times\sum_n\phi_n(z')\int dz''\phi_n^{\dagger}(z'')U_{\mathbf{g}}(z'')\Psi_0(z''), \tag{13}$$

where

$$a=\frac{im}{\hbar^2\kappa}\,\frac{1}{\hbar^2k_{\mathbf{g}}^2/2m-\epsilon_0+i\Gamma_{\rm in}/2}. \tag{14}$$

We consider the structure of the solution of this integral equation via an iterative method and take the zeroth-order solution as

$$\Psi_0^{(0)}(z)=\theta(-z)\exp(ik_0z)+\theta(z)\exp(i\kappa z), \tag{15}$$

where $\theta(z)$ is the unit step function. The zeroth-order approximation entails a semi-infinite crystal characterized by its potential (through κ) without the surface resonance phenomena. Inserting this into the right-hand side of Eq. (13), we obtain the first-order solution

$$\Psi_0^{(1)}(z)=\exp(i\kappa z)-a\sum_n\int dz'\exp(i\kappa|z-z'|)\times U_{-\mathbf{g}}(z')\phi_n(z')\int dz''\exp(i\kappa z'')U_{\mathbf{g}}(z'')\phi_n^{\dagger}(z''), \tag{16}$$

and inserting this back into Eq. (13), the second-order solution is obtained in a similar manner:

$$\Psi_0^{(2)}(z)=\Psi_0^{(1)}(z)+a^2\sum_n\int dz'\exp(i\kappa|z-z'|)\times U_{-\mathbf{g}}(z')\phi_n(z')\sum_{n'}\int dz''\int dz'''U_{\mathbf{g}}(z'')\times\phi_n^{\dagger}(z'')\exp(i\kappa|z''''-z'''|)U_{-\mathbf{g}}(z''')\phi_{n'}(z''')\times\int dz''''\exp(i\kappa z'''')U_{\mathbf{g}}(z'''')\phi_n^{\dagger}(z''''). \tag{17}$$

Inspection of the above equation reveals that to all orders the series can be constructed by the two factors

$$\int dz'\exp(i\kappa|z-z'|)U_{-\mathbf{g}}(z')\phi_n(z') \tag{18}$$

(and its conjugate; with a real potential, the conjugate of $U_{-\mathbf{g}}$ is $U_{\mathbf{g}}$) and

$$\int dz\int dz'U_{\mathbf{g}}(z)\phi_n^{\dagger}(z)\exp(i\kappa|z-z'|)U_{-\mathbf{g}}(z')\phi_{n'}(z'). \tag{19}$$

Since $\phi_n(z)$ is localized at the plane $z_n=nd$ we assume that $\exp(i\kappa|z-z'|)$ is approximately constant over the range of $\phi_n(z)$ and factor it out of the z' integration in Eq. (18), reducing Eq. (18) to

$$\exp(i\kappa|z-nd|)\Lambda_n. \tag{20}$$

Here we have defined following Dudarev and Whelan[12]

$$\Lambda_n=\int dz'U_{-\mathbf{g}}(z')\phi_n(z') \tag{21}$$

and the corresponding conjugate as

$$\Lambda_n^{\dagger}=\int dz'U_{\mathbf{g}}(z')\phi_n^{\dagger}(z'). \tag{22}$$

Here Λ_n ($\Lambda_n^\dagger$) is interpreted as the amplitude for the capture (emission) of the scattering electron by the localized Bloch state.

Following this viewpoint Eq. (19) can be viewed as the emission of the electron at z by the nth site, its propagation from z to z', and its subsequent capture at z' by the n'th site. Again due to the localized nature of the Bloch states, if $n \neq n'$, Eq. (19) reduces to $\exp(\kappa|n-n'|d)\Lambda_n^\dagger\Lambda_{n'}$. For $n=n'$ such an approximation is an oversimplification and we retain the form of Eq. (19), labeling it as M_n. Thus to second order, the wave function can be written as

$$\begin{aligned}\Psi_0^{(2)}(z) &= \exp(i\kappa z) - a\sum_n |\Lambda_n|^2 \exp(i\kappa|z-nd|)\exp(i\kappa nd)\\ &\quad + a^2\sum_n |\Lambda_n|^2\exp(i\kappa|z-nd|)\Bigg(M_n\exp(i\kappa nd)\\ &\quad + \sum_{n'(n'\neq n)} |\Lambda_{n'}|^2 \exp(i\kappa|n-n'|d)\exp(i\kappa n'd)\Bigg). \end{aligned} \tag{23}$$

To all orders, a solution for $\Psi_0(z)$ can be written as

$$\Psi_0(z) = \exp(i\kappa z) - \sum_n \exp(i\kappa|z-nd|) f_n, \tag{24}$$

where

$$\begin{aligned} f_n &= a|\Lambda_n|^2\Bigg[\exp(i\kappa nd) - a\Bigg(M_n\exp(i\kappa nd)\\ &\quad + \sum_{n_1(n_1\neq n)} \exp(i\kappa|n-n_1|d)\exp(i\kappa n_1 d)|\Lambda_{n_1}|^2\Bigg)\\ &\quad + a^2\Bigg(M_n\exp(i\kappa nd) + \sum_{n_1(n_1\neq n)}\\ &\quad \times\exp(i\kappa|n-n_1|d)\exp(i\kappa n_1 d)|\Lambda_{n_1}|^2\Bigg)\\ &\quad \times\Bigg(M_{n_1}\exp(i\kappa nd) + \sum_{n_2(n_2\neq n_1)}\\ &\quad \times\exp(i\kappa|n_1-n_2|d)\exp(i\kappa n_2 d)|\Lambda_{n_2}|^2\Bigg) + \cdots\Bigg]. \end{aligned} \tag{25}$$

Inspection of the above equation reveals that f_n satisfies the recurrence equation

$$\begin{aligned} f_n &= a|\Lambda_n|^2\Bigg[\exp(i\kappa nd) - \sum_{n_1(n_1\neq n)} \exp(i\kappa|n-n_1|d) f_{n_1}\Bigg]\\ &\quad + aM_n f_n, \end{aligned} \tag{26}$$

that is,

$$f_n = \frac{a|\Lambda_n|^2}{1-aM_n}\Bigg[\exp(i\kappa nd) - \sum_{n_1(n_1\neq n)} \exp(i\kappa|n-n_1|d) f_{n_1}\Bigg]. \tag{27}$$

With Λ_n and M_n taken as being the same for each lattice site, Eq. (27) reduces to a discrete version of the Weiner-Hopf integral equation,[19] indicating that there indeed exists an analytical solution to the problem at hand. In the present work this assumption is retained and the substitutions $|\Lambda_n|^2=\Lambda^2$ and $M_n=M$ are made,[20] giving

$$f_n = \frac{a\Lambda^2}{1-aM}\Bigg[\exp(i\kappa nd) - \sum_{n_1(n_1\neq n)} \exp(i\kappa|n-n_1|d) f_{n_1}\Bigg]. \tag{28}$$

Apart from a factor, this is essentially identical (albeit in a slightly different form) to the discrete integral equation developed by Dudarev and Whelan.

Note that in Eqs. (11)–(24), we have assumed that $z>0$ and thus used the Green's function defined in Eq. (8). For the scattering problem at hand, we are concerned with the solution of $\Psi_0(z)$ in the region $z<0$, and Eq. (24) can be rewritten as

$$\Psi_0(z) = \exp(ik_0 z) - R_{\text{res}}\exp(-ik_0 z), \tag{29}$$

where R_{res} is the elastic reflection coefficient given by

$$R_{\text{res}} = -\sum_n \exp(i\kappa nd) f_n. \tag{30}$$

IV. DEVIATIONS FROM THE BREIT-WIGNER SCATTERING FORMULA

For a single scatterer at $n=0$, the resonance reflection coefficient reduces to

$$R_{\text{res}} = \frac{-a\Lambda^2}{1-aM} \tag{31}$$

giving

$$R_{\text{res}} = -\frac{im}{\hbar^2 k_0}\,\frac{\Lambda^2}{\hbar^2 k_{\mathbf{g}}^2/2m - \epsilon_0 + \Gamma_{\text{in}}/2 + - im/\hbar^2 k_0 M}, \tag{32}$$

which is of the Breit-Wigner form, with the on-site self-energy term M due to the self-scattering mechanism.

In the strong attenuation limit (i.e., $\operatorname{Im}\kappa \gg 1/d$), the discrete integral equation for f_n reduces to

$$f_n = \frac{-a\Lambda^2}{1-aM}\exp(i\kappa nd) \tag{33}$$

giving the reflection coefficient as

$$\begin{aligned} R_{\text{res}} &= \frac{-a\Lambda^2}{1-aM}\sum_n \exp(i2\kappa nd) = \frac{-a\Lambda^2}{1-aM}\,\frac{1}{1-\exp(i2\kappa d)}\\ &\approx \frac{-a\Lambda^2}{1-aM}. \end{aligned} \tag{34}$$

Thus, as expected, an array of noninteracting scatterers reduces to the Breit-Wigner law. To consider deviations away from this simple form for (arbitrarily) weak attenuation, we generate the series solution for R_{res} by iterating Eq. (28), giving

$$R_{\rm res}=\frac{-a\Lambda^2}{1-aM}\sum_{nn'}\overline{G_{nn'}}\exp(i\kappa(n+n')d)$$
$$=\frac{-a\Lambda^2}{1-aM}\sum_{nn'}G_{0n}\overline{G_{nn'}}G_{n'0}, \tag{35}$$

where

$$\overline{G_{nn'}}=\delta_{nn'}-b\sum_{n_1(n_1\neq n)}G_{nn_1}\Bigg[\delta_{n_1n'}-b\sum_{n_2(n_2\neq n_1)}$$
$$\times G_{n_1n_2}\Bigg(\delta_{n_2n'}-b\sum_{n_3(n_3\neq n_2)}G_{n_2n_3}\cdots\Bigg)\Bigg]. \tag{36}$$

Here $G_{nn'}=\exp(i\kappa|n-n'|d)$ and $b=a\Lambda^2/(1-aM)$.

Thus the reflection coefficient can be expressed as a perturbation expansion with respect to the Breit-Wigner scattering vertex. To first order then, the reflection coefficient reduces to

$$R_{\rm res}=\frac{-a\Lambda^2}{1-aM}\frac{1}{1-\exp(i2\kappa d)}, \tag{37}$$

which is precisely the strong attenuation limit obtained earlier, Eq. (34). Thus, if $|a\Lambda^2/(1-aM)|$ is within the radius of convergence of the series in Eq. (36), to order $|a\Lambda^2/(1-aM)|^2$, the reflection coefficient exhibits simple Breit-Wigner scattering modified by the constant $1/[1-\exp(i2\kappa d)]$.

Higher-order contributions to the resonant reflection coefficient can also be easily evaluated. For example, the next-order term can be found by evaluating the second term in Eq. (35) and inspection of Eq. (36) reveals the second-order contribution to the reflection coefficient to be

$$R_{\rm res}=\left(\frac{a\Lambda^2}{1-aM}\right)^2\sum_{nn'(n'\neq n)}\exp(i\kappa nd)$$
$$\times\exp(i\kappa|n-n'|d)\exp(i\kappa n'd). \tag{38}$$

This can also be easily evaluated giving

$$R_{\rm res}=\left(\frac{a\Lambda^2}{1-aM}\right)^2\left(\frac{2\exp(i2\kappa d)}{[1-\exp(i2\kappa d)]^2}\right). \tag{39}$$

The reflection coefficient in its present form [Eq. (35)] has a simple interpretation; see Fig. 1. The lowest-order contribution is constructed from the sum over all sites of $G_{0n}(-b)G_{n'0}$, each of which represents the propagation from the surface to the site n, a resonant scatter (of the Breit-Wigner form) at n, and propagation back to the surface. Correspondingly the second-order contribution is then the sum of the site combinations n and n' $(n\neq n')$ of the term $G_{0n}(-b)G_{nn'}(-b)G_{n'0}$; the propagation from the surface to site n, a resonant scatter at n, propagation from n to n', a resonant scatter at n', and the propagation back to the surface.

Inspection of Eqs. (37) and (39) reveals that to second order, the nth-order coefficients in the expansion of R contain the factor $[1-\exp(i2\kappa d)]^{-n}$. It is not difficult to see that this is also the case for all higher-order terms since each internal summation will indirectly involve the $n=0$ to ∞ scattering vertices. Using the straightforward Cauchy definition for the radius of convergence, the radius of convergence for Eq. (36) will scale as $|1-\exp(i2\kappa d)|$ indicating nonconvergence of the developed representation at $\kappa d=N\pi$ (where $N=1,2,3,\ldots$), that is, at Bragg scattering angles perpendicular to the surface. An underlying assumption of the present model is that the scattering geometry is such that the scattering angle along this direction is in the off-Bragg regime; $\kappa d=(N+1/2)\pi$ (where $N=1,2,3,\ldots$). Thus in the present context, we expect Eq. (36) to be convergent if $|a\Lambda^2/(1-aM)|<|1-\exp(i2\kappa d)|$.

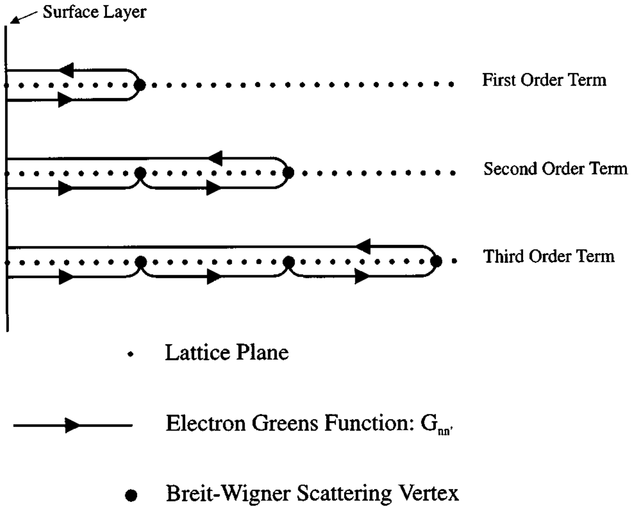

FIG. 1. A diagrammatic representation of the surface resonance reflection coefficient to third order in the Breit-Wigner scattering vertex. The first-order term consists of a ‘‘free’’ propagation from the surface to a particular lattice plane, followed by a Breit-Wigner scatter, and then a propagation back to the surface; the Breit-Wigner scattering vertex contains all possible self-scattering events within the intermediate plane. The first-order reflection coefficient is then given by a summation over all such lattice planes. The second- and third-order terms have a similar interpretation where now each summation excludes the starting lattice plane, which has already been taken into account via the Breit-Wigner scattering vertex.

V. APPLICATION TO PLATINUM

Comparison between RHEED experiments and computations have met with considerable success for the platinum (111) surface.[21] Following Dudarev and Whelan,[12] we consider incident 100 keV electrons on the platinum (111) surface at glancing angles satisfying the off-Bragg scattering condition for the two **g** vectors (440) and (220). In each case, for the range of azimuthal angles considered, the energy $\hbar^2k_{\mathbf{g}}^2/2m$ can be negative and therefore $k_{\mathbf{g}}$ an evanescent wave propagating in a direction parallel to the surface. At $T=293$ K, the relevant 1D Bloch state [in the laterally averaged potential of the (111) planes] is the lowest band which ranges in energy between 65.75 eV and 65.68 eV. This indicates an essentially dispersionless band that can be successfully parametrized by a 1D nearest-neighbor tight-binding Hamiltonian with an on-site energy (ϵ_0) of -65.72 eV and a bandwidth of 0.037 eV. The inelastic bandwidth of this state

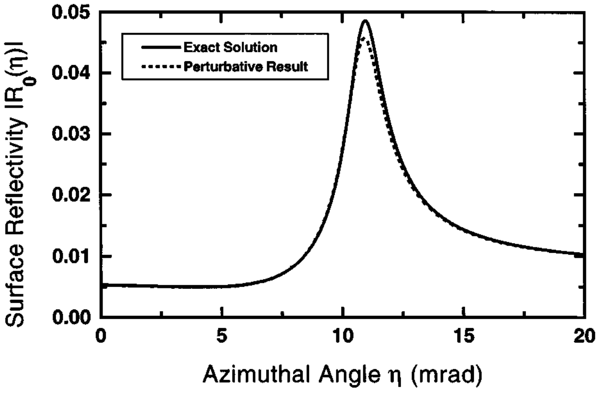

FIG. 2. The surface reflectivity near resonance for the $(\bar{4}40)$ direction using the exact result and first-order perturbative result. The parameters used were $M=2.3+i0.4$ eV and $(m/\hbar^2\kappa)\Lambda^2=0.6+i0.6$ eV.

(Γ) can be regarded as constant and equal to 18.85 eV.

The total reflection coefficient is the sum of the resonant part and the potential part. For the present scattering geometry, the potential part (primarily a function of the glancing angle) is taken to be $R_{\mathrm{pot}}=(1.3032+i7.062\,12)\times10^{-3}$ for both **g** vectors.

Figures 2 and 3 display the magnitude of the sum of the resonant and potential reflection coefficient, as a function of azimuthal angle [the zero azimuthal angle corresponds to the $[\bar{1}\bar{1}2]$ azimuth of the (111) surface] for the **g** vectors $\bar{4}40$ and $\bar{2}20$, respectively. We plot both the first-order result, using Eq. (37), and the exact result determined by Dudarev and Whelan.[12] For Fig. 2, the $\bar{4}40$ case, the first-order perturbative result differs from the exact result by no more than 6%, whereas in Fig. 3, the $\bar{2}20$ geometry, the perturbative result differs by up to 8%. We note that to second order, using Eq. (39), there is no discernible difference between the exact result and the perturbative result on the scale chosen.

Mathematically this is simply due to the smallness of the magnitude of the simple Breit-Wigner scattering vertex. For the $\bar{4}40$ case it is approximately 0.04 at resonance, indicating a 4–5% accuracy when using only the lowest-order term. For the $\bar{2}20$ case at resonance, the magnitude is approximately 0.10, indicating a 10% accuracy when using the first-order result. Upon inspection of Figs. 2 and 3 we see that this is indeed the case.

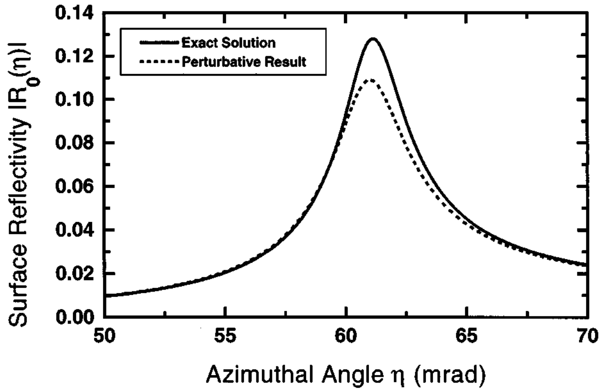

FIG. 3. The surface reflectivity near resonance for the $(\bar{2}20)$ direction vector using the exact result and first-order perturbative result. The parameters used were $M=7.5+i0.84$ eV and $(m/\hbar^2\kappa)\Lambda^2=1.5+i1.0$ eV.

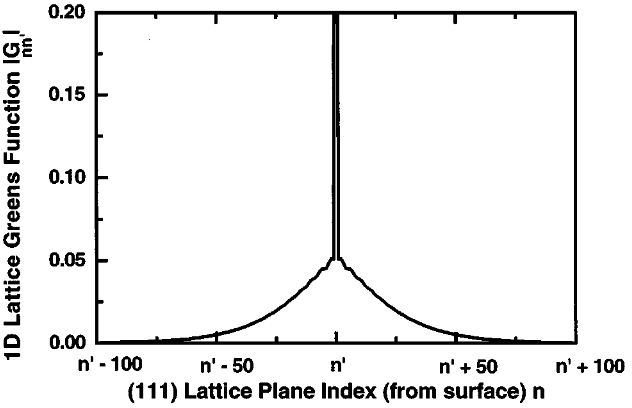

FIG. 4. The magnitude of the resonant Green's function, Eq. (36), connecting n to n' (set equal to 500 to remove the effect of the surface) (111) planes. This is evaluated for the $(\bar{4}40)$ scattering direction at resonance ($\eta\approx12$ mrad).

What perhaps is surprising at first is that the perturbation expansion gives such a result, that is, the presumed complicated interference effect of the semi-infinite lattice produces little deviation of the reflection coefficient from the simple Breit-Wigner scattering law. Indeed the imaginary part of the crystal momentum, κ, indicates that the scattering process is highly nonlocal; in the present regime it ranges up to 50 lattice planes from the surface.

The origin of this phenomenon can be seen in the radius of convergence scaling approximately as $|1-\exp(i2\kappa d)|$, indicating a complete breakdown of the present expansion at Bragg scattering angles, while on the other hand, a well-behaved series [provided $|a\Lambda^2/(1-aM)|<|1-\exp(i2\kappa d)|$] at off-Bragg scattering angles. This is simply due to the (111) component of the wave vector κ not being a reciprocal-lattice vector for the scattering geometries chosen, an inherent assumption of the present model in order to ignore potential scattering (the electron diffraction effect). Nevertheless, since the resonance vertex *is periodic* in the (111) direction, the interference effect occurring in the higher-order multiple scattering processes is largely incoherent, thus not contributing significantly to deviations away from the Breit-Wigner form.

The incoherent nature of the scattering between planes becomes manifest upon inspection of $|G_{nn'}|$, the square of which can be viewed as an unnormalized probability connecting planes n and n'. Figure 4 displays $|G_{nn'}|$ for a given n far from the surface and a corresponding range for n'. Inspection reveals that at $n=n'$, $|G_{nn'}|=1$, due to the first Kronecker δ term in Eq. (36). Beyond this, there exists an essentially smooth function, the limit of which, when approaching $n'=n$, does not approach unity. This represents the general effect of incoherent scattering—a dominant nonscattering term superimposed on a much smaller background amplitude. Note that this essential feature remains when considering $|G_{nn'}|$ closer to the surface.

Thus for platinum and the scattering geometry used, the present form of resonant scattering can be regarded as approximately arising from a semi-infinite array of noninteracting Breit-Wigner scatterers. Indeed since the vertex amplitudes M and Λ (as well as κ) are only known to within 10% and, moreover, are varied to achieve an adequate fit, it can be said that the underlying physics still remains that of the Breit-Wigner form, since our first-order result is also to within less than 10% of the exact result.

VI. EXTENSION TO THE STRONG POTENTIAL SCATTERING REGIME

The present perturbation expansion breaks down for strong Bragg potential scattering perpendicular to the surface and the exact solution for the reflection coefficient is needed. In this regime where a horizontal Kikuchi line intersects a resonance parabola, the potential scattering must now be treated on an equal footing. In a subsequent paper, Dudarev and Whelan[15] employ a more realistic electron Green's function derived from 1D bulk Bloch wave functions. In this case, the discrete integral equation for f_n becomes

$$f_n=\frac{a\Lambda^2\tau v}{1-aM}\left[\exp(i\kappa nd)-\sum_{n_1(n_1\neq n)}\left(\exp(i\kappa|n-n_1|d)-\frac{\rho}{v}\exp\big(i\kappa(n+n_1)d\big)\right)f_{n_1}\right], \tag{40}$$

where now

$$\Lambda=\int dz\, b(z,\kappa)U_{-\mathbf{g}}(z)\phi_n(z) \tag{41}$$

and

$$\int dz\int dz' U_{\mathbf{g}}(z)\phi_n^{\dagger}(z)G\left(z,z',\frac{\hbar^2K_0^2}{2m}\right)U_{-\mathbf{g}}(z')\phi_{n'}(z'). \tag{42}$$

Here Eqs. (41) and (42) (via the Green's function) use the 1D Bloch function $b(z,\kappa)$ corresponding to an electron with energy $\hbar^2K_0^2/2m$, the solution to Eq. (5). In Eqs. (40)–(42) there exist the parameters τ, v, and ρ, all of which characterize the surface region and bulk potential properties (see Dudarev and Whelan[15]) of the semi-infinite crystal.

Inspection of Eq. (40) reveals that $\exp(i\kappa nd)$ can be factored out of the second term in the n_1 summation. Using standard resummation techniques, the resulting series expansion for the total reflection coefficient can then be written as

$$R_{\text{res}}=\frac{-\tau\Sigma_n\exp(i\kappa nd)g_n}{v+\rho\Sigma_n\exp(i\kappa nd)g_n}, \tag{43}$$

where

$$g_n=\frac{a\Lambda^2\tau v}{1-aM}\left[\exp(i\kappa nd)-\sum_{n_1(n_1\neq n)}\exp(i\kappa|n-n_1|d)g_{n_1}\right], \tag{44}$$

which is of a similar form to Eq. (28). Such a result also follows naturally from the exact solution.[15] Thus the effect of potential scattering on the resonance scattering reflection coefficient can be dealt with exactly, with or without knowledge of the exact solution of the ''purely'' resonance contribution. We note that the so-called ''purely'' resonance term, contained in Eq. (44), does also depend on the potential scattering in a simple way, via the renormalized vertices M and $\Lambda\tau v$.

We thus have an expression for the reflection coefficient which is essentially exact with respect to the potential scattering mechanism, and in the present context, perturbative with respect to resonant scattering. This immediately suggests that a suitable criterion in which a perturbation expansion in terms of the (renormalized) Breit-Wigner scattering vertex remains valid for arbitrarily large potential scattering is

$$\frac{a\Lambda^2\tau v}{1-aM}<|1-\exp(2i\kappa d)|. \tag{45}$$

Here the scattering vertices are now given by Eqs. (41) and (42).

VII. BEYOND THE ''TWO ROD'' APPROXIMATION

In the present section we investigate the application of the convergence criterion beyond the ''two rod'' approximation. To generalize the present formalism to N rods we must return to the full Schrödinger equation [Eq. (1)] from which a series of coupled integral equations can be obtained:

$$\Psi_0(z)=\Psi^{+}_{k_0}(z)-\sum_{\mathbf{g}'\neq 0}\int dz' G\left(z,z',\frac{\hbar^2k_0^2}{2m}\right)\times U_{-\mathbf{g}'}(z')\Psi_{\mathbf{g}'}(z'), \tag{46}$$

$$\Psi_{\mathbf{g}}(z)=\sum_{\mathbf{g}'\neq\mathbf{g}}\int dz' G\left(z,z',\frac{\hbar^2k_{\mathbf{g}}^2}{2m}\right)U_{\mathbf{g}-\mathbf{g}'}(z')\Psi_{\mathbf{g}'}(z'),\qquad \mathbf{g}\neq 0. \tag{47}$$

From the procedure outlined at the beginning of Sec. III, these equations must be transformed to a single integral equation in terms of the specular wave function $\Psi_0(z)$. Inspection of the above reveals that for an N-rod approximation, where $N>2$, the lowest order of such an integral equation will be infinite. This can be demonstrated for the case of $N=3$ in which Eqs. (46) and (47) reduce to three coupled integral equations [for notational brevity, we now write the electron Green's function as $G_{\mathbf{h}}(z,z')$, where $\mathbf{h}$ can be zero or an arbitrary two-dimensional reciprocal-lattice vector],

$$\Psi_0(z)=\Psi^+_{k_0}(z)+\int dz' G_0(z,z')U_{-\mathbf{g}_1}(z')\Psi_{\mathbf{g}_1}(z')$$
$$+\int dz' G_0(z,z')U_{-\mathbf{g}_2}(z')\Psi_{\mathbf{g}_2}(z'), \tag{48}$$

$$\Psi_{\mathbf{g}_1}(z)=\int dz' G_{\mathbf{g}_1}(z,z')U_{\mathbf{g}_1}(z')\Psi_0(z')$$
$$+\int dz' G_{\mathbf{g}_1}(z,z')U_{\mathbf{g}_1-\mathbf{g}_2}(z')\Psi_{\mathbf{g}_2}(z'), \tag{49}$$

$$\Psi_{\mathbf{g}_2}(z)=\int dz' G_{\mathbf{g}_2}(z,z')U_{\mathbf{g}_2}(z')\Psi_0(z')$$
$$+\int dz' G_{\mathbf{g}_2}(z,z')U_{\mathbf{g}_2-\mathbf{g}_1}(z')\Psi_{\mathbf{g}_1}(z'). \tag{50}$$

Here $\Psi_{\mathbf{g}_2}(z)$ can be eliminated by substituting Eq. (50) into Eqs. (48) and (49), giving

$$\Psi_0(z)=\Psi^+_{k_0}(z)+\int dz' G_0(z,z')U_{-\mathbf{g}_1}(z')\Psi_{\mathbf{g}_1}(z')+\int dz' G_0(z,z')U_{-\mathbf{g}_2}(z')\int dz'' G_{\mathbf{g}_2}(z',z'')U_{\mathbf{g}_2}(z'')\Psi_0(z'')$$
$$+\int dz' G_0(z,z')U_{-\mathbf{g}_2}(z')\int dz'' G_{\mathbf{g}_2}(z',z'')U_{\mathbf{g}_2-\mathbf{g}_1}(z'')\Psi_{\mathbf{g}_1}(z''), \tag{51}$$

$$\Psi_{\mathbf{g}_1}(z)=\int dz' G_{\mathbf{g}_1}(z,z')U_{\mathbf{g}_1}(z')\Psi_0(z')+\int dz' G_{\mathbf{g}_1}(z,z')U_{\mathbf{g}_1-\mathbf{g}_2}(z')\int dz'' G_{\mathbf{g}_2}(z',z'')U_{\mathbf{g}_2}(z'')\Psi_0(z'')$$
$$+\int dz' G_{\mathbf{g}_1}(z,z')U_{\mathbf{g}_1-\mathbf{g}_2}(z')\int dz'' G_{\mathbf{g}_2}(z',z'')U_{\mathbf{g}_2-\mathbf{g}_1}(z'')\Psi_{\mathbf{g}_1}(z''). \tag{52}$$

The right-hand side of Eq. (52) is still a function of $\Psi_{\mathbf{g}_1}(z)$, which upon repeated substitution into Eq. (51) produces a integral equation for $\Psi_0(z)$ of infinite order.

In the present work we consider the coupling between resonance parabolas arising from two evanescent propagation modes parallel to the surface characterized, in part, by the vectors **g** and $-\mathbf{g}$. By virtue of such resonance parabolas appearing distinctly separate in typical experimental and numerical RHEED spectra, the coupling between two such modes must in general be weak and therefore it seems, for now, a good approximation to consider only the linear coupling terms contained in Eqs. (51) and (52). Substituting Eq. (52) into (51), with $\mathbf{g}_1=\mathbf{g}$ and $\mathbf{g}_2=-\mathbf{g}$, and discarding higher-order terms (beyond linear) in $U_{\mathbf{g}_2-\mathbf{g}_1}(z'')=U_{\pm 2\mathbf{g}}(z'')$, gives a third-order integral equation entirely in terms of $\Psi_0(z)$:

$$\Psi_0(z)=\Psi^+_{k_0}(z)+\int dz' G_0(z,z')U_{-\mathbf{g}}(z')\int dz'' G_{\mathbf{g}}(z',z'')U_{\mathbf{g}}(z'')\Psi_0(z'')+\int dz' G_0(z,z')U_{\mathbf{g}}(z')$$
$$\times\int dz'' G_{-\mathbf{g}}(z',z'')U_{-\mathbf{g}}(z'')\Psi_0(z'')+\int dz' G_0(z,z')U_{-\mathbf{g}}(z')\int dz'' G_{\mathbf{g}}(z',z'')U_{2\mathbf{g}}(z'')$$
$$\times\int dz''' G_{-\mathbf{g}}(z'',z''')U_{-\mathbf{g}}(z'')\Psi_0(z)+\int dz' G_0(z,z')U_{\mathbf{g}}(z')$$
$$\times\int dz'' G_{-\mathbf{g}}(z',z'')U_{-2\mathbf{g}}(z'')\int dz''' G_{\mathbf{g}}(z'',z''')U_{\mathbf{g}}(z'')\Psi_0(z). \tag{53}$$

Here the first three terms correspond to two independent resonance modes and the last two terms contain their mutual interaction. To consider the form of the interaction terms, we substitute the explicit form of the resonant Green's function [Eq. (10)] into the last term (say) of Eq. (53):

$$\int dz' G_0(z,z')\frac{\Sigma_n\phi_n(z')U_{\mathbf{g}}(z')}{\hbar^2k^2_{-\mathbf{g}}/2m-\epsilon_0+i\Gamma_{\text{in}}/2}\,\frac{\Sigma_{n'}\int dz''\phi^\dagger_n(z'')U_{-2\mathbf{g}}(z'')\phi_{n'}(z'')}{\hbar^2k^2_{\mathbf{g}}/2m-\epsilon_0+i\Gamma_{\text{in}}/2}\int dz'''\phi^\dagger_{n'}(z''')U_{\mathbf{g}}(z''')\Psi_0(z'''). \tag{54}$$

It is the integral, $\int dz\phi^\dagger_n(z)U_{2\mathbf{g}}(z)\phi_{n'}(z)$, which couples the two modes together and due to the localized nature of $\phi_n(z)$ can be approximated as $\delta_{n,n'}\int dz|\phi_n(z)|^2U_{2\mathbf{g}}(z)$, reducing Eq. (54) to

$$\int dz' G_0(z,z')\frac{\Sigma_n\phi_n(z')U_{\mathbf{g}}(z')T_{\mathbf{g},n}}{(\hbar^2k^2_{-\mathbf{g}}/2m-\epsilon_0+i\Gamma_{\text{in}}/2)}\int dz'''\phi^\dagger_n(z''')U_{\mathbf{g}}(z''')\Psi_0(z'''), \tag{55}$$

where we have defined

$$T_{\mathbf{g},n}=\frac{1}{(\hbar^2k_{\mathbf{g}}^2/2m-\epsilon_0+i\Gamma_{\mathrm{in}}/2)}\int dz|\phi_n(z)|^2U_{-2\mathbf{g}}(z). \tag{56}$$

Thus the integral equation for $\Psi_0(z)$ [Eq. (53)] reduces to

$$\Psi_0(z)=\Psi_{k_0}^{+}(z)+\int dz'\,G_0(z,z')\sum_n \phi_n(z')\int dz''\,\phi_n^{\dagger}(z'')\left(\frac{U_{-\mathbf{g}}(z')U_{\mathbf{g}}(z'')}{\hbar^2k_{\mathbf{g}}^2/2m-\epsilon_0+i\Gamma_{\mathrm{in}}/2}+\frac{U_{\mathbf{g}}(z')U_{-\mathbf{g}}(z'')}{\hbar^2k_{-\mathbf{g}}^2/2m-\epsilon_0+i\Gamma_{\mathrm{in}}/2}\right.$$
$$\left.+\frac{U_{-\mathbf{g}}(z')T_{-\mathbf{g}}U_{-\mathbf{g}}(z'')}{\hbar^2k_{\mathbf{g}}^2/2m-\epsilon_0+i\Gamma_{\mathrm{in}}/2}+\frac{U_{\mathbf{g}}(z')T_{\mathbf{g}}U_{\mathbf{g}}(z'')}{\hbar^2k_{-\mathbf{g}}^2/2m-\epsilon_0+i\Gamma_{\mathrm{in}}/2}\right)\Psi_0(z''), \tag{57}$$

where $T_{\mathbf{g}}=T_{\mathbf{g},n}$; that is, each plane is again regarded as equivalent. We note that (both) the interaction terms become a maximum for an incident electron direction in which the two resonance parabola intersect; i.e., when both $\hbar^2k_{\mathbf{g}}^2/2m$ and $\hbar^2k_{-\mathbf{g}}^2/2m$ are equal to ϵ_0.

From a diagrammatic perspective, Eq. (57) has a simple interpretation. The first two terms [ignoring $\Psi_{k_0}^{+}(z)$] correspond to independent resonance modes ($\mathbf{g}$ and $-\mathbf{g}$) and therefore involve the capture and release of an electron at a particular plane. The remaining interaction terms will involve the capture by a mode, say $\mathbf{g}$, its transferral to the other mode, $-\mathbf{g}$, via the amplitude $T_{\mathbf{g}}$, and its release from that mode. Due to the approximation outlined between Eqs. (54) and (55), these processes all occur on the same plane.

To investigate the perturbative solution, we set $T_{\mathbf{g}}$ to zero and note that Eq. (57) then corresponds to two independent resonance modes. The solution for the resonant reflection coefficient can then be immediately written down as

$$R_{\mathrm{res}}=\frac{-(a_{\mathbf{g}}\Lambda_{\mathbf{g}}\Lambda_{\mathbf{g}}^{\dagger}+a_{-\mathbf{g}}\Lambda_{-\mathbf{g}}\Lambda_{-\mathbf{g}}^{\dagger})}{1-a_{\mathbf{g}}M_{\mathbf{g},\mathbf{g}}-a_{-\mathbf{g}}M_{-\mathbf{g},-\mathbf{g}}}\sum_{nn'} G_{0n}\overline{G_{nn'}}G_{n'0}, \tag{58}$$

where $\overline{G_{nn'}}$ is defined in an analogous manner to Eq. (36) of Sec. IV (with b suitably redefined). In the above we have used the following definitions:

$$a_{\mathbf{g}}=\frac{im}{\hbar^2\kappa}\left(\frac{1}{\hbar^2k_{\mathbf{g}}^2/2m-\epsilon_0+i\Gamma_{\mathrm{in}}/2}\right), \tag{59}$$

$$\Lambda_{\mathbf{g}}=\int dz'\,U_{-\mathbf{g}}(z')\phi_n(z'), \tag{60}$$

and

$$M_{\mathbf{g},\mathbf{g}'}=\int dz\int dz'\;U_{\mathbf{g}}(z)\phi_n^{\dagger}(z)$$
$$\times\exp(i\kappa|z-z'|)U_{-\mathbf{g}'}(z')\phi_{n'}(z'). \tag{61}$$

The generalization to nonzero $T_{\mathbf{g}}$, for the resonant reflection coefficient, then becomes clear:

$$R_{\mathrm{res}}=\frac{-(a_{\mathbf{g}}\Lambda_{\mathbf{g}}\Lambda_{\mathbf{g}}^{\dagger}+a_{-\mathbf{g}}\Lambda_{-\mathbf{g}}\Lambda_{-\mathbf{g}}^{\dagger}+a_{\mathbf{g}}T_{\mathbf{g}}\Lambda_{\mathbf{g}}\Lambda_{-\mathbf{g}}^{\dagger}+a_{-\mathbf{g}}T_{-\mathbf{g}}\Lambda_{-\mathbf{g}}\Lambda_{\mathbf{g}}^{\dagger})}{1-a_{\mathbf{g}}M_{\mathbf{g},\mathbf{g}}-a_{-\mathbf{g}}M_{-\mathbf{g},-\mathbf{g}}-a_{\mathbf{g}}T_{\mathbf{g}}M_{\mathbf{g},-\mathbf{g}}-a_{-\mathbf{g}}T_{-\mathbf{g}}M_{\mathbf{g},-\mathbf{g}}}\sum_{nn'} G_{0n}\overline{G_{nn'}}G_{n'0}, \tag{62}$$

where Eqs. (59)–(61) still apply and b is again suitably redefined in $G_{nn'}$ [Eq. (36)].

Thus, under the linear coupling approximation, the convergence criterion developed in Secs. IV and VI remains intact, albeit slightly modified. At first glance, the approximation of linearity in the coupling seems essential for this to be the case. This is in fact incorrect. Indeed, the underlying approximation for the convergence criterion to remain valid is entailed in the coupling integral, $\int dz\,\phi_n(z)U_{2\mathbf{g}}(z)\phi_{n'}^{\dagger}(z)$, being approximated as $\delta_{n,n'}\int dz|\phi_n(z)|^2U_{2\mathbf{g}}(z)$; that is, allowing interactions between modes to occur only on the same plane. Thus, under this approximation, the inclusion of (higher-order) couplings between modes simply renormalizes the fundamental scattering vertex at each plane; the interplane scattering mechanism remaining unchanged. This result is easily generalized to a higher number of interacting "rods."

VIII. DISCUSSION AND CONCLUDING REMARKS

The present viewpoint, developed by Dudarev and Whelan, indicates that in the regime considered, the resonance parabolas encountered in the RHEED technique arise primarily from the interaction of the incident electron with bulk electronic states. Such a statement is of course canonical in the present context due to the localized nature of the electronic states probed by the scattering geometries considered; the surface as such does not play a dynamical role since it does not effect the electronic structure. Furthermore in the present model the surface plane is indistinguishable from that of the bulk.

In the simplest case, the addition of surface structure to the present model would take the form of a modification to the Breit-Wigner scattering vertex for the surface plane(s) (for example, the simplest case is at $n=0$) and/or the lattice spacing between the surface planes. The physical origin may be a true ''reconstruction'' of the localized surface state (albeit minor in the case of platinum), a crude average due to weak surface roughness or physisorption. Again for platinum such an effect would be minor due to the states (and indeed the surface states[22]) near the Fermi level playing the primary role in any surface chemistry phenomenon, whereas the states considered in the present work are tightly bound and high above the Fermi level. In any event, such a representation for deviations from the atomically flat case can be at best regarded as a crude approximation, for it assumes that the resonant Green's function retains its form at the surface plane; a fortuitous assumption. Nevertheless, to deviate as little as possible from the present model, such an approximation is briefly considered.

The perturbation expansion for the resonant reflection coefficient [Eq. (35); in these preliminary considerations we only investigate the case of weak potential scattering] can be easily modified to admit a different surface term. If we label the surface Breit-Wigner scattering vertex as s and the bulk as b, it is not difficult to see that the first-order resonant reflection coefficient becomes $R_{\mathrm{res}}=s+b\exp(i2\kappa d)/[1-\exp(i2\kappa d)]$, which is linear in s. It turns out that this linearity in s is retained if we consider the next term in the expansion of R, an important result for platinum since we needed only to go to second order to obtain a result almost identical to the exact calculation; note we assume both s and b are of similar order. Thus the effect of surface structure on the resonance reflection coefficient is linear in the present regime. The realization of such a relation in the experimental realm would allow a simple ''extraction'' of the surface structure if the atomically flat case could also be experimentally realized.

In the present formalism, the general problem of surface roughness (which may include stepped surfaces or surface islands) has been associated with the same difficulties encountered in the numerical approaches to calculating RHEED spectra. If disorder occurs over a range of scales, a simple average of the surface roughness will no longer suffice; higher-order correlation functions are needed to describe the disorder and the mean of the surface becomes an ill-defined quantity due to strong fluctuations. Under these circumstances, a straightforward two-dimensional Fourier decomposition of the Schrödinger equation [Eq. (1) in Sec. II] is no longer justified and any ensuing method of solution is untenable. In this case, a new approach must be developed, such as a dynamical treatment of the fluctuating component of the crystal potential.[23] We note, however, that even under these conditions, if the localized nature of the in-plane states is still maintained, then the mechanism of coherent and incoherent scattering between the planes will still be of prevalence. Thus the general structure of the perturbation theory—apart from the on-plane scattering vertex which could have a significantly different form and vary from plane to plane—developed here is retained.

In conclusion, the pioneering work of Dudarev and Whelan has been reexpressed in terms of a perturbation series with respect to a simple Breit-Wigner scattering vertex. For the case of weak potential scattering in platinum, the exact expression for the resonant reflection coefficient can be replaced by the lowest-order term to within the uncertainties of the scattering parameters—the primary scattering mechanism still being that of the Breit-Wigner form. From an analysis of the convergence properties and the full interplane resonant electronic Green's function, this has been shown to arise from incoherent scattering between the planes, a result of the underlying assumption of the minimal potential scattering approximation. For these very reasons, in the case of strong potential scattering, the perturbation expansion is expected to break down and the exact expression for the resonant reflection coefficient must be utilized. The intermediate regime between weak and strong potential scattering has nevertheless been investigated from a perturbative perspective and a resulting convergence criterion developed. The general formalism is also found to be applicable to the interacting many-rod problem when the underlying assumption of strongly localized states is retained.

ACKNOWLEDGMENTS

The authors wish to thank Dr. S. L. Dudarev for providing the numerical values from his platinum calculation and to acknowledge the financial assistance of the Australian Research Council Small Grant Scheme.

---

[1] Z. L. Wang, *Reflection Electron Microscopy and Spectroscopy for Surface Analysis* (Cambridge University Press, Cambridge, 1996).

[2] P. Hirsch *et al.*, *Electron Microscopy of Thin Crystals* (Butterworths, London, 1965).

[3] Z. L. Wang, *Elastic and Inelastic Scattering in Electron Diffraction and Imaging* (Plenum Press, New York, 1995), pp. 23–35.

[4] See, for example, Ref. 1, Chap. 4.

[5] S. Kikuchi and S. Nakagawa, Sci. Pap. Inst. Phys. Chem. Res. **21**, 256 (1933).

[6] S. Miyake and K. Hayakawa, Acta Crystallogr. A **26**, 60 (1970).

[7] Z. L. Wang, Rep. Prog. Phys. **56**, 997 (1993).

[8] E. G. McRae, Surf. Sci. **25**, 491 (1971).

[9] E. G. McRae, Rev. Mod. Phys. **51**, 541 (1979).

[10] K. Kambe, Surf. Sci. **20**, 213 (1970).

[11] L.-M. Peng, Surf. Sci. **316**, L1049 (1994).

[12] S. L. Dudarev and M. J. Whelan, Surf. Sci. **310**, 373 (1994).

[13] S. L. Dudarev and M. J. Whelan, Phys. Rev. Lett. **72**, 1032 (1994).

[14] S. L. Dudarev and M. J. Whelan, Int. J. Mod. Phys. B **10**, 133 (1996).

[15] S. L. Dudarev and M. J. Whelan, Surf. Sci. **340**, 293 (1995).

[16] See, for example, Ref. 3, Chap. 5.

[17] See, for example, A. Gonis, *Green's Functions for Ordered and*

Disordered Systems (North-Holland, Amsterdam, 1992), Chap. XX, pp. 599–636. See also Ref. 18, Chaps. 4–7.

[18] E. N. Economou, *Green's Functions in Quantum Physics*, 2nd ed. (Springer-Verlag, Berlin, 1983), p. 5.

[19] P. M. Morse and H. Feshbach, *Methods of Theoretical Physics* (McGraw-Hill, New York, 1953), Part I, pp. 978–992.

[20] This definition differs slightly from the work of Dudarev and Whelan (Ref. 12), who define M as Eq. (19) multiplied by $im/\hbar^2\kappa$.

[21] A. E. Smith, G. Lehmpfuhl, and Y. Uchida, Ultramicroscopy **41**, 367 (1992).

[22] P. Roos, E. Bertel, and K. D. Rendulic, Chem. Phys. Lett. **232**, 537 (1995).

[23] Z. L. Wang, Surf. Sci. **366**, 377 (1996).